Vincamine as a Potential Therapeutic Agent for Sickle Cell Disease: A Comprehensive Computational Study

Basumatary Nerswn[1], Chetia Pankaj[2], Baruah Chittaranjan[3] and Sarmah Jatin[1]*
1. Department of Biotechnology, Bodoland University, Kokrajhar, Assam, 783370, INDIA
2. Department of Life Sciences, Dibrugarh University, Dibrugarh, Assam, 786004, INDIA
3. P.G. Department of Zoology, Darrang College, Tezpur, Assam, 784001, INDIA
*jatinsarmahindia@gmail.com

Abstract
Sickle cell disease refers to a hereditary blood condition, characterized by the presence of abnormally shaped erythrocytes resulting from a singular point mutation in the β-globin gene, causing various health complications. At present, hydroxyurea remains the sole pharmacological agent for sickle cell disease management, despite its adverse effects. This investigation examines 64 naturally occurring compounds, documented to exhibit anti-sickling properties as alternative to hydroxyurea, using computational techniques. In this research, molecular docking was utilized to assess the binding affinity of 64 natural compounds with haemoglobin S, along with ADME analysis to determine drug-likeness and pharmacokinetic profiles of the compounds, followed by molecular dynamics and binding free energy calculations to evaluate stability of the protein-ligand complex.

Based on the outcomes of molecular docking and ADME analysis, vincamine was identified to possess favourable binding affinity and passed necessary pharmacokinetic criteria. Molecular dynamics simulations and free energy assessments indicated that vincamine-HbS complex maintained stability, exhibiting moderate flexibility and compactness. The combined approach of molecular docking, ADME and molecular dynamics simulations highlights vincamine as a promising candidate for the therapeutic intervention of sickle cell disease. Additional experimental validations, both in vitro and in vivo, are however necessary to validate the anti-sickling effectiveness of vincamine.

Keywords: Sickle cell disease, Anti-sickling, Molecular docking, MD simulation, ADME.

Introduction

Sickle cell disease (SCD) refers to a hereditary blood condition, leading to around 300,000 new SCD cases identified each year in new-borns[3,27]. India is the nation with the second highest prevalence of SCD affected new-borns[3,26]. SCD refers to an inherent condition that leads to the production of irregular shaped red blood cells which can lead to a number of health issues. SCD is triggered by one point mutation originating in the β-globin gene (HBB) which causes switching of glutamic acid with valine at the sixth position of the polypeptide chain[11,13]. Due to this change in the β-globin gene, formation of haemoglobin S (HbS) occurs. Under low oxygen circumstances haemoglobin S (HbS) polymerizes, resulting in the erythrocytes to take a firm, sickle-like structure[25].

The clinical symptoms associated with SCD exhibit considerable heterogenity, extending from acute vaso-occlusive crises, which are notably marked by intense pain as well as long term complications that include organ impairment and shortened life expectancy[28]. Upon deoxygenation, HbS molecules form hydrophobic bonds between the valine on one polypeptide and various amino acids on adjacent chains, notably phenylalanine, alanine and leucine. These interactions trigger polymerization which produces a stiff structure around 20 nm in diameter. This process induces the precipitation of HbS molecules within erythrocytes, leading to the morphological alteration of these cells into a deformed sickled configuration[12]. Furthermore, the presence of chronic haemolytic anaemia, which is a defining feature of SCD, plays an important role in the development of systemic complications[14].

The therapies involving stem cell and bone marrow transplantation are characterized not only by their sky-high expenses but also by challenges associated with the compatibility between donors and recipients. For erythrocyte-related disorders, hydroxyurea (HU) serves as the primary pharmacological agent by promoting the synthesis of foetal haemoglobin (HbF) production. HU is routinely utilized in the clinical management of SCD. Nonetheless, HU serves as a harmful substance that causes programmed cell death in late-stage erythroid progenitor cells leading to reduction in ribonucleotide reductase activity, S-phase cytotoxicity and obstructs both DNA production and repair functions. Additionally, it exerts an effect on RNA and protein biosynthesis.

As a result of its cytotoxic properties, some patients may exhibit inadequate response to HU and experience side effects[29]. Current therapeutic approaches for SCD are inadequate and predominantly focus on symptom relief and complication management, rather than tackling the principal aetiology of the condition[33]. Medicinal plants demonstrate substantial therapeutic capabilities and are employed in the treatment of several ailments. They present a direct, economically viable strategy for disease management[1,5,21,24]. An observable growth through the scholarly examination of

surrounding phytochemicals, particularly the secondary metabolites from plants, has emerged as potential therapeutic agents for a number of diseases, including SCD.

Secondary metabolites obtained from plants, identified for their various bioactive properties, provide a promising avenue for the development of novel anti-sickling agents. These compounds have demonstrated efficacy in stabilizing haemoglobin, reducing oxidative stress and inhibiting the polymerization of deoxygenated HBS, thereby alleviating the pathophysiological effects associated with SCD[2]. Numerous extracts from diverse medicinal plants have demonstrated anti-sickling properties; however, a highly effective pharmacological intervention for the management of SCD continues to remains elusive[5].

Molecular docking and molecular dynamics (MD) simulations have emerged as sophisticated computational methodologies for examining the interactions and stability between small molecules and biological macromolecules at the atomic scale. Molecular docking enables the calculation of the preferred binding conformation of a ligand to its biological target whereas MD simulations provide insights about the dynamic behaviour and stability of the protein-ligand complex throughout its interaction[20]. These methodologies are pivotal in elucidating the mechanistic basis of the anti-sickling effects exhibited by plant derived secondary compounds and in identifying promising candidates for subsequent experimental validation.

This research endeavour is designed to utilize molecular docking and MD simulation techniques to examine the anti-sickling efficacy of various selected plant derived secondary metabolites. Through the examination of their interactions with HbS as well as their dynamic stability, this investigation seeks to enhance the understanding of the molecular mechanisms that reinforce their therapeutic effects and to identify potential lead compounds for the formulation of effective treatments for SCD.

Material and Methods

Compound Retrieval: For this study, 64 natural compounds that have been reported for having anti-sickling properties, have been collected from available literature and database[8].

Protein Structure Preparation: The crystallographic configuration of carbonmonoxy haemoglobin S (HbS) in complex with GBT440 (PDB ID: 5E83) was retrieved from the Protein Data Bank (PDB) online repository accessible at http://www.rcsb.org. Heteroatoms, aqueous molecules, the ligand co-crystallized in the form of (2-methyl-3-({2-[1-(propan-2-yl)-1H-pyrazol-5-yl]pyridin-3-yl}methoxy) phenol), along with supplementary solvent molecules, were removed from the structure utilizing the BIOVIA Discovery Studio visualization software. Polar hydrogen atoms and Kollman united charges were incorporated using version 1.5.7 of Auto Dock Tools (ADT). Non-polar hydrogen atoms were amalgamated and the docking input file (PDBQT) was generated with ADT. The protein was oriented via docking in a rigid conformation without the occurrence of protein relaxation.

Ligand Structure Preparation: A comprehensive total of 64 phytochemical metabolites exhibiting anti-sickling properties were systematically retrieved from existing literature for the current investigation. Ligands were obtained in a three-dimensional structure from the PubChem Database. The ligand files obtained, were subsequently translated into Protein Data Bank (PDB) file format utilizing Open Babel software version 3.1.1. Within the AutoDock Tools (ADT), Gasteiger charges were integrated into the ligands, while non-polar hydrogen atoms were amalgamated, ultimately resulting in the arrangement of aromatic carbons, rigid scaffolds and flexible linkages, after which the files were preserved in PDBQT file format for docking purposes. The ligands were afforded torsional flexibility to exhibit a diverse range of orientations and structural adaptability.

Active site and grid generation: We defined a grid box, surrounding the described binding position of haemoglobin affinity modulators, in the locality N-terminal (valine1) of the alpha subunit of the Hb S protein. The co-crystallized ligand bound to residues at this site, was 2-methyl-3- {[2-(1-(propan-2-yl)-1H-pyrazol-5-yl)pyridin-3-yl]methoxy} phenol. The dimensions of the grid box along the X, Y and Z axes were established at 126, 126 and 126 respectively, with an interstitial spacing of 0.375 Angstrom between the grid points. A central grid box for the coordinates X, Y and Z was established at the values 20, 5 and 20 respectively.

Molecular Docking: The Auto Dock Vina[30] software was employed to predict energetically favourable binding orientations between the selected ligands and the HbS protein. The docking procedure was carried out on a cohort of 64 phytochemicals that were of particular significance. A local search global optimization algorithm was utilized to perform the docking, while the Broaden-Fletcher-Goldfarb-Shanno (BFGS) method was implemented to enable local optimization. Moreover, this methodology functioned as a positive control within the docking experiment. By setting a docking exhaustiveness parameter to 8, the software produced 9 poses of the protein-ligand complex which were thereafter organized according to their binding affinity.

Data pertaining to the root mean square deviation (rmsd) for the upper boundary (rmsdu b.) and lower boundary (rmsdl b.) of the binding conformations were evaluated. The docking positions were prioritized according to their binding affinity, with the conformation displaying the highest binding affinity chosen for further investigation. The docking sites were systematically ranked in accordance with their binding affinity and the conformation exhibiting the most significant binding affinity was selected for additional investigation. The configuration and alignment of the

binding sites, in conjunction with the involved amino acids, bond types and bond lengths, were analysed utilizing the BIOVIA discovery studio visualizer.

Drug Likeness and ADME analysis: The Swiss ADME[4] analytical tool was utilized for the evaluation of the pharmacodynamics of the small molecules under investigation, displaying maximum affinity of binding, accompanied by a binding conformation that closely resembles to that of the bound ligand GBT440. The assessment of the ligands was further conducted, taking into account their physicochemical characteristics including lipophilicity and solubility in water. Pharmacokinetic properties were evaluated in relation to their gastrointestinal (GI) absorption and permeability across the Blood-Brain Barrier (BBB). The drug likeness was assessed on the basis of their deference with the criteria established by Lipinski et al[16], Ghose et al[10], Veber et al[32], Egan et al[6] and Muegge et al[22] and principles of medicinal chemistry based on their compliance with lead likeness.

Molecular Dynamics Simulation: The Gromacs-2019.4[31]software tool was utilized to conduct molecular dynamics simulations on the chosen protein-ligand complex. To acquire the requisite coordinates for the force field, the optimal ligand topology was sourced from the ATB repository. The system was established for 1500 steps with vacuum minimization using the steepest descent procedure. Subsequently, utilizing a simple point charge (SPC) water model, the intricate structures were dissolved within a cubic periodic lattice measuring 0.5 nm. The intricate systems were then retained at an appropriate molarity of 0.15 M of salt through careful addition of the necessary quantities of chloride (Cl^-) counter ions and sodium (Na^+) ions.

The last production run for each resultant structure derived from the NTP equilibration stage was conducted within the NTP ensemble for a simulation period of 100 ns[9]. A specific procedure utilizing the GROMACS simulation suite for analysing protein RMSD, RMSF, RG, SASA and H-bond was employed to examine the trajectory.

Binding Free Energy Calculation: The Molecular Mechanics Poisson-Boltzmann surface area (MM-PBSA) approach[19] was applied to understand the compound's binding free energy (ΔG binding) with the protein during the simulation period. We evaluated the protein's binding free energy with the hit compound using the GROMACS function g_mmpbsa[15]. The binding free energy of the compound was calculated using the formula:

$$\Delta G_{binding} = \Delta G_{complex} - (\Delta G_{protein} + \Delta G_{ligand})$$

where $\Delta G_{complex}$ denotes free energy of protein-ligand complex, $\Delta G_{protein}$ denotes free energy of protein and ΔG_{ligand} denotes free energy of the ligand.

Results

Molecular Docking: The findings from the molecular docking of probable anti-sickling compounds are displayed in table 1. Using Autodock Vina, the molecular interactions of 64 active compounds with the carbonmonoxyHbS protein were investigated. Each docking run produced nine docking conformations, which were ranked using the software's pre-established scoring criteria in accordance with their affinity of binding.

The ligands that showed highest affinity of binding were Apigenin, B Sitosterol, Barbaloin, Biflavanone, Cajanin, Carotenoid, Cassane Furanoditerpene, Catechin, Cepharantine, Chamuvaritin, Coleon U, Emodin, Epicatechin, Epigallocatechin gallate, Isovitexin, Kolaviron, Lupeol, Pfaffic acid, Piperine, Rutin, Stigmasterol, Uvarinol, Vincamine, Vitexin with binding affinities of -8.1, -9.1, -8.1, -10.2, -8.3, -9.7, -9.2, -8, -11.5, -9.1, -8.3, -7.8, -8.1, -9.1, -8.4, -9.9, -10.4, -10.5, -8.5, -9.9, -9.3, -10.9, -9.2 and -9.2 Kcal/mol correspondingly. The interaction between these compounds and the target protein was visualized using Biovia Discovery Studio and Chimera. Among these compounds, vincamine exhibited a comparable interaction with the co-crystallized ligand GBT440 which is a haemoglobin-oxygen modulator[7,18,23].

Table 1
Binding affinity of 64 natural compounds docked with sickled haemoglobin (HbS) along with their molecular weight obtained from our previous study.

S.N.	Compound Name	Binding Affinity (Kcal/mol)	Molecular Weight (g/mol)
1	2-hydroxymethyl benzoic acid	-6.6	152.15
2	3,4-dihydroxybenzoic acid	-5.9	154.12
3	4 hydroxybenzoic acid	-6.4	138.12
4	4-flurobenzoic acid	-6.3	140.11
5	Allantoin	-6	158.12
6	Apigenin	-8.1	270.05
7	Arginine	-6	174.2
8	Ascaridole	-6.4	168.23
9	Ascorbic acid	-5.5	176.12
10	B Sitosterol	-9.1	414.71

11	Barbaloin	-8.1	418.4
12	Benzaldehyde	-5.5	106.12
13	Benzoic acid	-6.1	122.12
14	Biflavanone	-10.2	446.5
15	Caffeine	-6	194.19
16	Cajanin	-8.3	300.26
17	Carotenoid	-9.7	568.9
18	Caryophylene	-7	204.35
19	Cassane Furanoditerpene	-9.2	340.5
20	Catechin	-8	290.27
21	Cepharantine	-11.5	606.7
22	Chamuvaritin	-9.1	452.5
23	Chryseriol	-7.8	300.26
24	Chrysophanol	-7.7	254.24
25	Coleon U	-8.3	346.4
26	Diallyl disulphide	-3.4	146.3
27	Emodin	-7.8	270.24
28	Epicatechin	-8.1	290.27
29	Epigallocatechin gallate	-9.1	450.4
30	Eugenol	-6.3	164.2
31	Eugenyl acetate	-6.1	206.24
32	Fagaramide	-7.4	247.29
33	Fagaronine	-7.9	350.4
34	Flavan-3-ol	-7.3	226.27
35	Isoplumbagin	-6.6	188.18
36	Isovitexin	-8.4	432.4
37	Kampferol	-7.8	286.24
38	Kolaviron	-9.9	588.50
39	Leucine	-5.5	131.17
40	Lupeol	-10.4	426.70
41	Lysine	-5.6	146.19
42	M-coumaric acid	-6.4	164.16
43	O-vanillin	-5.3	170.16
44	P-coumaric acid	-6.5	164.16
45	P-cymene	-6.6	134.22
46	Pellitorine	-6	223.35
47	Pfaffic acid	-10.5	440.70
48	Phenylalanine	-6.3	165.19
49	Piperine	-8.5	285.34
50	Plumbagin	-6.8	188.18
51	Quercitin	-8.4	302.23
52	Rutin	-9.9	610.50
53	Serine	-4	105.09
54	Stigmasterol	-9.3	412.70
55	Tryptophan	-6.7	204.22
56	Tyrosine	-6.8	181.19
57	Uvarinol	-10.9	574.60
58	Valine	-5.2	117.15
59	Vanillic acid	-5.8	168.15
60	Vavain glucoside	-7.1	492.40
61	Vavain	-8	344.30
62	Vincamine	-9.2	354.40
63	Vitexin	-9.2	354.40
64	Zanthoxylol	-7.2	220.31

ADME Analysis of compounds: Swiss ADME server was used to analyse the ADME properties of vincamine, based on the results obtained from molecular docking. Vincamine passes the ADME filters (Lipinski, Ghose, Veber, Egan and Muegge filters) with bioavailability score of 0.55. Table 2 displays the results of vincamine's ADME parameters.

Molecular Dynamics: Vincamine-haemoglobin complex was subjected to molecular dynamics simulation in order to examine the stability of the vincamine-haemoglobin complex in a dynamic system over a 100ns time frame. The parameters adopted included root mean square deviation (RMSD), root mean square fluctuation (RMSF), radius of gyration (Rg), hydrogen bond (H-bond), solvent accessible surface area (SASA) and binding free energy (MMPBSA).

The vincamine-HbS complex displayed an average RMSD of 0.23 ± 0.02 nm from 0 to 100 ns, indicating relative stability during simulation. The complex remained steady throughout the simulation. To evaluate the stability of the Cα atoms and residues, RMSF was determined for the complex. The RMSF measurements were calculated against the simulation timescale of 0 to 100 ns and the average RMSF for the complex was found to be 0.12 ± 0.07 nm.

Table 2
ADME profile of Vincamine obtained from Swiss ADME server

S.N.	ADME Parameters	Compound's score
Physicochemical parameter		
1	Canonical SMILES	COC(=O)C1(O)CC2(CC)CCCN3C2c2n1c1ccccc1c2CC3
2	Formula	$C_{21}H_{26}N_2O_3$
3	Molecular weight	354.44
4	Number of heavy atoms	26
5	Fraction Csp3	0.57
6	Number of aromatic heavy atoms	9
7	Number of rotatable bonds	3
8	Number of H-bond acceptors	4
9	Number of H-bond donors	1
10	Molar refractivity	103.74
11	TPSA	54.7
Lipophilicity		
12	Log Po/w(iLOGP)	2.81
13	Log Po/w(XLOGP3)	2.86
14	Log Po/w(WLOGP)	2.14
15	Log Po/w(MLOGP)	2.62
16	Log Po/w(SILICOS-IT)	2.6
17	Consensus log P o/w	2.61
Pharmacokinetics		
18	GI absorption	High
19	BBB permeant	Yes
20	P-Gp permeant	Yes
21	CYP1A2 inhibitor	No
22	CYP2C19 inhibitor	No
23	CYP2C9inhibitor	No
24	CYP3A4inhibitor	No
25	Log Kp (skin permeation)	-6.43
Drug likeness		
26	Lipinski	0, violation
27	Ghose	0, violation
28	Veber	0, violation
29	Egan	0, violation
30	Muegge	0, violation
31	Bioavailability score	0.55
Medicinal chemistry		
32	Pains	0 alert
33	Brenk	0 alert
34	Lead likeness	1 violations
35	Synthetic accessibility	4.49

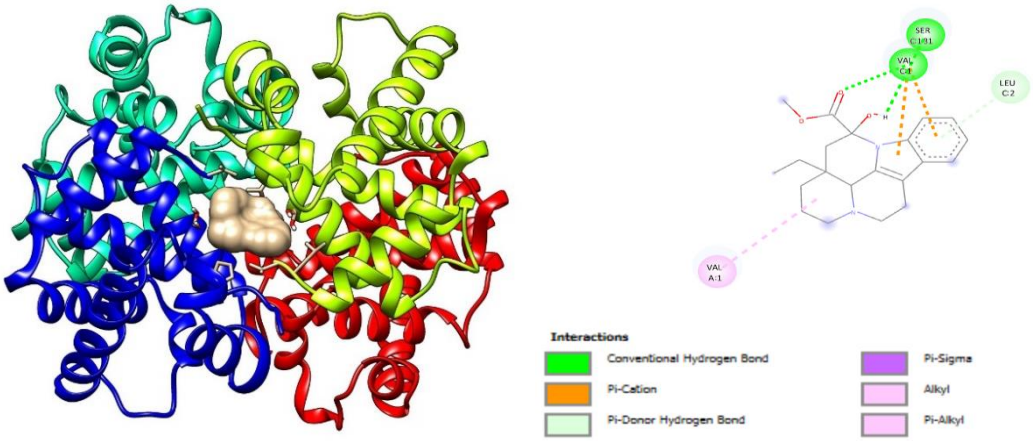

Figure 1: Image on the left represents the docked pose and orientation of Vincamine complexed with HbS (PDB ID: 5E83). Image on the right represents 2D interaction of vincamine docked with HbS.

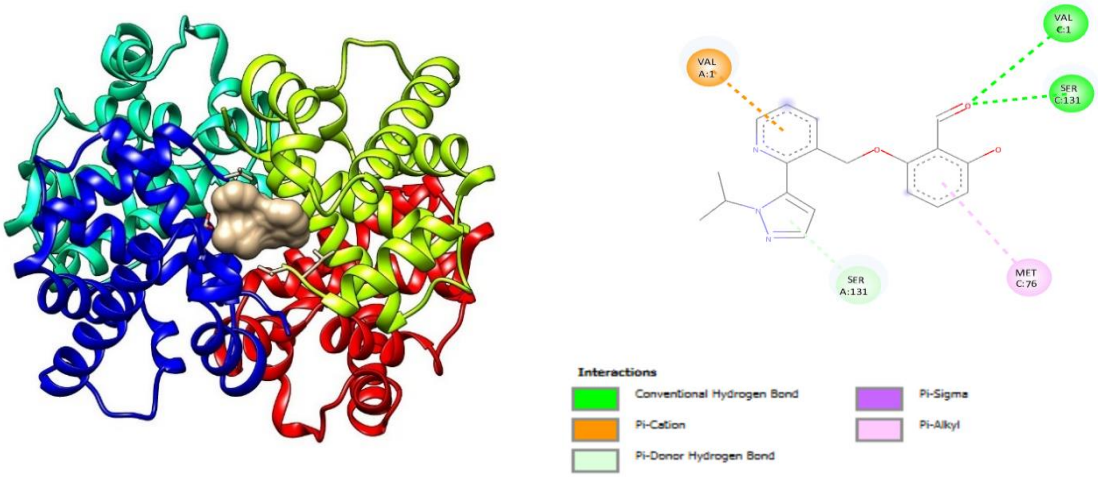

Figure 2: Image on the left represents the docked pose and orientation of GBT440 complexed with HbS (PDB ID: 5E83). Image on the right represents 2D interaction of GBT440 docked with HbS.

To investigate the compactness of the vincamine-HbS complex during the simulation, the Radius of Gyration was determined. The complex exhibited an average Rg value of 1.48 ± 0.01 nm throughout the simulation time. Intermolecular hydrogen bonding formed during molecular docking was further investigated to demonstrate the hydrogen bonding pattern of the vincamine-HbS complex. The hydrogen bonding pattern is displayed in figure 3 (E).

Furthermore, the fluctuations in SASA values were analysed to assess the compactness of the hydrophobic core. The complex displayed an average SASA value of 75.38 ± 2.84 nm^2 from 0 to 100 ns time frame, suggesting no variation in structural level protein during the simulation.

Binding Free Energy: Relative binding free energy of the vincamine-HbS complex was acquired from MMPBSA calculations. The relative binding free energy ($\Delta G_{binding}$) for the complex was -27.190 ± 23.750 kJ/mol. The values for electrostatic energy, Van der Waal energy, SASA energy and polar solvation energy were -53.653 ± 28.466 kJ/mol, -123.123 ± 7.581 kJ/mol, -14.177 ± 0.383 kJ/mol and 163.763 ± 45.697 kJ/mol respectively.

Discussion

Sickle cell disease (SCD) refers to a hereditary blood condition, leading to around 300,000 new SCD cases identified each year in new-borns[3,27]. India is the nation with the second highest prevalence of SCD affected new-borns[3,26]. In conditions characterized by low oxygen saturation, polymerization of HbS occurs within the erythrocytes, resulting in the structural alteration of these cells, which subsequently leads to severe, sometimes fatal crises[17]. To this day, hydroxyurea is the only medication recommended by the FDA for the management of SCD, with its mechanism of action not fully known[29]. *In vitro* assessments targeting the anti-sickling properties of various plant extracts have been undertaken in previous studies.

However, the investigation into the efficacy of the bioactive compounds present within these extracts has been notably restricted. Therefore, the application of *in silico* approaches

for the exploration and development of more effective anti-sickling agents derived from plant extracts is necessary for the adequate handling of SCD.

Upon reviewing earlier research studies on anti-sickling property of different plant extracts, 64 compounds were found to be relevant for the current study. Molecular docking study was then carried out to assess the interaction of these compounds with sickled haemoglobin. After analysis of interaction of the compounds with the target protein, vincamine was found to exhibit similar pattern of interaction like the co-crystallized ligand GBT440, which is an orally bioavailable R-state stabilizer of HbS[18]. Vincamine interacts with Val C:1, Ser C:131, ValA:1 and LeuC:2 of the HbS molecule.

On the other hand, GBT440 interacts with Val A:1, Val C:1, SerC:131, Ser A:131, Met C:76. The interactions observed between the two compounds as common amino acids (Val C:1, Val A:131, Ser C:131) are found to interact with these compounds, indicating that vincamine may possess functions similar to that of GBT440 (Figure 1 and 2). The development of H-bond with Val A:1 and Ser C:131 in combination with Val C:1 of the α chain of haemoglobin, appears to constitute a significant interaction for the preservation of R-state of HbS[18]. This suggests that vincamine may exhibit similar properties like GBT440 for maintaining the R-state of HbS and delay the process of polymerization. Upon re-docking with HbS, GBT440 exhibited a docking score of -7.3 Kcal/mol.

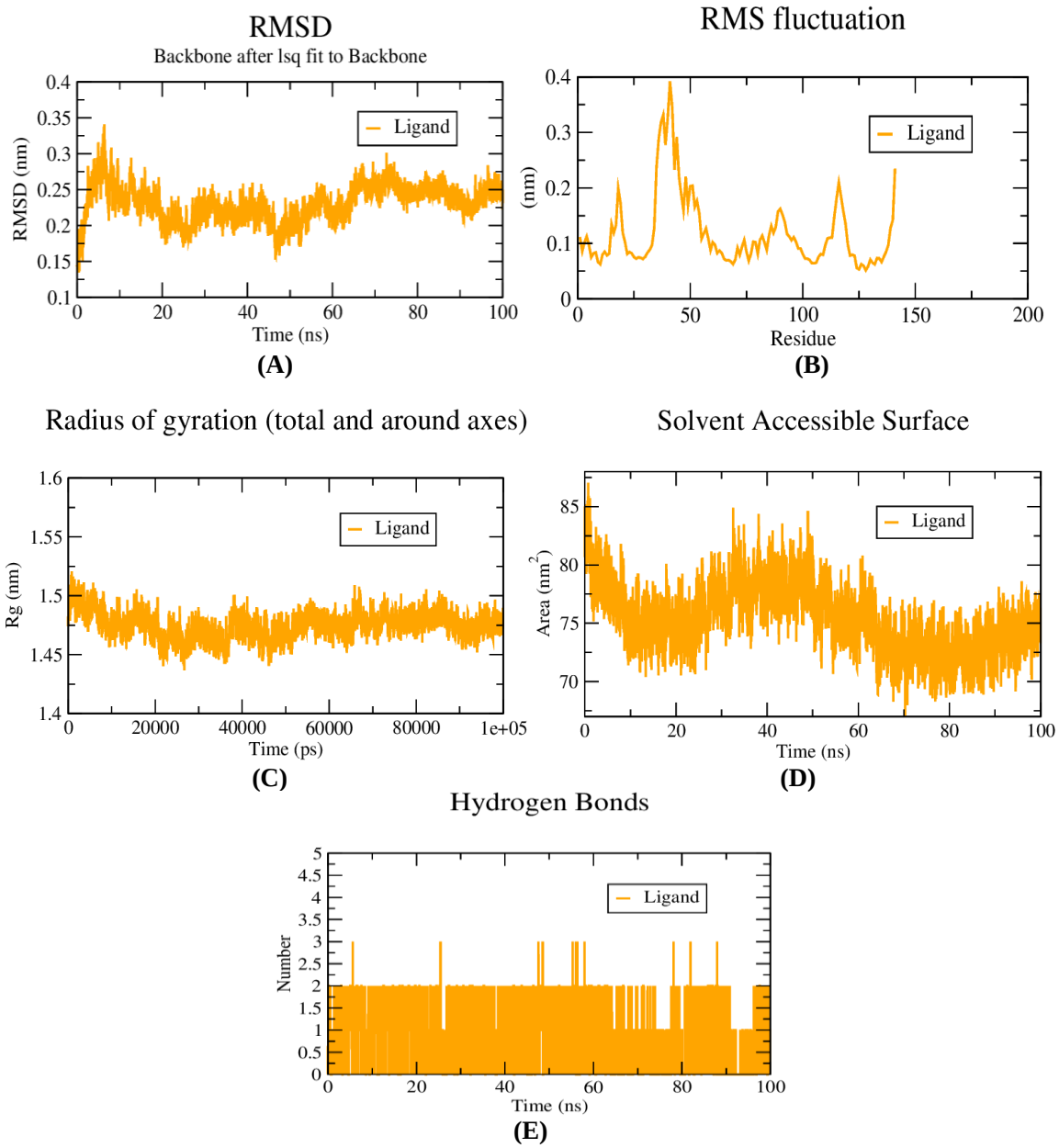

Figure 3: (A) RMSD plot of Vincamine-HbS complex during molecular dynamics simulation; (B) RMSF plot based on MD simulation trajectory; (C) Rgplot of back bone atoms of Vincamine; (D) Changes in the number of hydrogen bonds between small molecules and proteins during the process of molecular dynamics simulation; (E) SASA of back bone atoms of Vincamine-HbS complex.

Vincamine, on the other hand, exhibited a docking score of -9.2 Kcal/mol, which is relatively higher compared to the docking score of GBT440, signifying that vincamine has better binding affinity towards HbS compared to GBT440.

The pharmacokinetic features regarding absorption, distribution, metabolism and excretion (ADME) of a biologically active molecule are closely associated to its physicochemical qualities. These crucial variables define the pharmacokinetic behaviour, toxicological implications and bioavailability profile of a pharmaceutical agent. To mitigate the risk of failure of novel therapeutics during their concluding stages of development, it is important that ADME considerations are integrated at the early stages of drug discovery and development workflow. The ADME characteristics of vincamine were evaluated using the Swiss ADME online platform. Vincamine positively cleared numerous essential criteria, comprising the Lipinski, Ghose, Veber, Egan and Muegge filters[6,10,16,22,32], which are crucial for evaluating the drug-like properties and pharmacological capability of a compound.

The bioavailability score of 0.55 for vincamine signifies a quantitative assessment derived from its physicochemical characteristics and adherence to the above mentioned filters, implying a moderate probability of vincamine's oral bioavailability. A bioavailability score of 1.0 represents high oral bioavailability, nevertheless, a score of 0.55 remains positive, suggesting that vincamine possesses an ample possibility of being absorbed effectively upon oral administration.

Based on the ADME characteristics of the compounds under investigation, vincamine was chosen for molecular dynamics simulations spanning a duration of 100 ns in order to evaluate the stability of the complex with the dynamic system. RMSD serves as an essential parameter in MD simulations by measuring the deviation of atomic coordinates of a protein from a reference structure as a function of time. Lower RMSD values typically indicate enhanced stability and less structural variability of the complex. The average RMSD for the complex was 0.23 ± 0.02 nm from 0 to 100 ns which indicated relative stability of the complex throughout the simulation period. The complex showed slight fluctuation in the beginning from 0 to 10 ns followed by minor fluctuations from 20 ns till 100 ns, with highest fluctuation of 0.35 nm at about 10 ns (Figure 3A). The RMSD plot indicates a relatively stable interaction between vincamine and HbS, suggesting that vincamine maintains a consistent binding pose within the HbS binding site throughout the simulation.

Examination of C-α atoms and their corresponding residues can be carried out with the RMSF graph. The RMSF parameter provides insights into the comprehensive structural flexibility exhibited by the C-α atoms of each residue within a given system, with higher values indicating increased atomic mobility. The average fluctuation of the C-α atoms in the complex was 0.12 ± 0.07 nm as shown in figure 3B. The analysis of RMSF plot indicates that the vincamine-HbS complex demonstrates a moderate degree of atomic flexibility. The average RMSF value of 0.12 nm, together with a relatively low standard deviation of ± 0.07 nm, signifies that vincamine interacts with HbS in a manner that sustains an optimal level of flexibility. This flexibility is critical for preserving the functional dynamics of HbS while concomitantly ensuring the stability of vincamine's binding.

To investigate the spatial compactness of vincamine-HbS complex during the MD simulation time frame, the Radius of Gyration was assessed. In a dynamic system, Rg serves as an indicator of the overall dimension of the protein and is employed in the calculation of RMSD by aggregating all atoms from its centre of mass. The spatial arrangement of the atoms within a protein or a protein-ligand complex around their centre of mass is measured by Rg which serves as an indicator of the overall compactness of the molecular structure. The complex had an average Rg value of 1.48 ± 0.01 nm as shown in figure 3C. The Rg plot showed almost linear graph with minor fluctuations, suggesting that the complex maintains a relatively compact conformation with minimal expansion or contraction over the simulation timeframe. The stability of the vincamine-HbS complex, indicated by a consistent Rg value, supports our RMSD and RMSF findings, which also suggest stable and moderately flexible interactions.

The SASA serves as acrucial tool for the assessment of folding dynamics throughout computational simulations. The value of SASA functions as an indicator of the accessible surface area of a biomolecule that is available to the surrounding molecules or solvent. A significantly large SASA value indicates that a majority of the protein molecule is exposed to the solvent and surrounding molecules. The average SASA value from 0 to 100 ns time for the complex was 75.38 ± 2.84 nm^2. This implies that although vincamine interacts with HbS, it may not entirely hinder solvent access to the protein as the protein comprises a large amount of surface area that is accessible to the solvent.

Hydrogen bonding is considered essential to stabilize the protein-ligand interaction in the dynamic system. The establishment of hydrogen bonds between the protein-ligand complex is illustrated in figure 3E. The observation of MD trajectory over a duration of 100 ns revealed the formation of numerous H-bonds, thereby demonstrating a strong interaction between the protein and ligand, resulting in the formation of a stable complex. The graph shows the number of hydrogen bonds fluctuating between 1 and 3, with an average of approximately 2 bonds being consistently maintained throughout the simulation.

The constant formation of H-bonds throughout the entire simulation period signifies a stable interaction between vincamine and HbS, implying that vincamine is likely to remain bound to HbS within physiological conditions.

One of the critical parameters in understanding the stability and binding affinity of a molecular complex is the binding free energy (BFE), denoted as$\Delta G_{binding}$. BFE was determined for vincamine-HbS complex through the application of MMPBSA methodology, utilizing a MD trajectory of 100 ns. The BFE for the vincamine-HbS complex was determined to be -27.190 ± 23.750 kJ/mol, thereby signifying a strong binding energy for the complex. The high negative total BFE suggests that the formation of the vincamine-HbS complex in a dynamic environment is favourable, thereby confirming the stability of the complex. The complex exhibits a higher cumulative binding energy, suggesting a better affinity towardsHbS.

The BFE calculations further revealed that the electrostatic, van der Waals and SASA energies play a crucial role in the formation of vincamine-HbS complex. The van der Waals energy plays a crucial role in the atomic interactions within the protein-ligand complex, preserving the complex's structural integrity and stability throughout the MD simulations. The van der Waals, electrostatic and SASA energies associated with the complex were determined to be -123.123 ± 7.581 kJ/mol, -53.653 ± 28.466 kJ/mol and -14.177 ± 0.383 kJ/mol respectively. The presence of a negative Van der Waals energy value suggests that non-covalent interactions such as dispersion forces and steric complementarity, play a substantial role in influencing the stability of the complex.

The results of SASA energy analysis further indicated that the formation of the complex leads to reduction in the solvent-accessible surface area, which is energetically favourable. Furthermore, the polar solvation energy was observed to exhibit a positive interaction with a value of 163.763 ± 45.697 kJ/mol. This finding is simply a strong and stable interaction of the vincamine-HbS complex, indicating the ligand exhibits a strong affinity for the protein at the binding site.

Conclusion

Vincamine was identified to possess favourable binding affinity with HbS, in addition to possessing suitable drug likeness and pharmacokinetic profile. Molecular dynamics simulation of vincamine-HbS complex has also demonstrated a stable interaction, exhibiting moderate flexibility at the atomic level and a compact structure of the complex, indicating its potential as a promising candidate for further exploration as anti-sickling agent. In conclusion, the stability and favourable interaction characteristics of the vincamine-HbS complex, in conjunction with its excellent pharmacokinetic properties, highlight its potential as a therapeutic agent for SCD.

Nevertheless, although the results obtained from MD simulations are promising, it is crucial to note that computational studies are merely one aspect of the comprehensive drug discovery process. Additional experimental validations, both *in vitro* and *in vivo*, are necessary to validate the anti-sickling effectiveness of vincamine.

Acknowledgement

We would like to express our sincere gratitude to the Bioinformatics Infrastructure Facility, Department of Biotechnology, Bodoland University, for their invaluable support and resources throughout this research. Their provision of advanced bioinformatics tools and technical assistance was instrumental in the successful completion of our study.

References

1. Ameh S.J., Tarfa F.D. and Ebeshi B.U., Traditional herbal management of sickle cell anemia: lessons from Nigeria, *Anemia*, **2012**, 607436 **(2012)**

2. Ataga K.I., Kutlar A., Kanter J., Liles D., Cancado R., Friedrisch J., Guthrie T.H., Knight-Madden J., Alvarez O.A., Gordeuk V.R., Gualandro S., Colella M.P., Smith W.R., Rollins S.A., Stocker J.W. and Rother R.P., Crizanlizumab for the Prevention of Pain Crises in Sickle Cell Disease, *The New England Journal of Medicine*, **376(5)**, 429–439 **(2017)**

3. Babu B.V., Sridevi P., Surti S., Ranjit M., Bhat D., Sarmah J., Sudhakar G. and Sharma Y., Inadequate community knowledge about sickle cell disease among the Indian tribal population: a formative assessment in a multicentric intervention study, *Transactions of the Royal Society of Tropical Medicine and Hygiene*, **115(12)**, 1434–1444 **(2021)**

4. Daina A., Michielin O. and Zoete V., SwissADME: a free web tool to evaluate pharmacokinetics, drug-likeness and medicinal chemistry friendliness of small molecules, *Scientific Reports*, **7**, 42717 **(2017)**

5. Dash B.P., Archana Y., Satapathy N. and Naik S.K., Search for antisickling agents from plants, *Pharmacognosy Reviews*, **7(13)**, 53–60 **(2013)**

6. Egan W.J., Merz K.M. Jr. and Baldwin J.J., Prediction of drug absorption using multivariate statistics, *Journal of Medicinal Chemistry*, **43(21)**, 3867–3877 **(2000)**

7. Ferrone F.A., GBT440 increases haemoglobin oxygen affinity, reduces sickling and prolongs RBC half-life in a murine model of sickle cell disease, *British Journal of Haematology*, **174(4)**, 499–500 **(2016)**

8. Folashade K.O. and Omoregie E.H., Chemical constituents and biological activity of medicinal plants used for the management of sickle cell disease-A review, *Journal of Medicinal Plants Research*, **7(48)**, 3452-3476 **(2013)**

9. Gangadharappa B.S., Sharath R., Revanasiddappa P.D., Chandramohan V., Balasubramaniam M. and Vardhineni T.P., Structural insights of metallo-beta-lactamase revealed an effective way of inhibition of enzyme by natural inhibitors, *Journal of Biomolecular Structure & Dynamics*, **38(13)**, 3757–3771 **(2020)**

10. Ghose A.K., Viswanadhan V.N. and Wendoloski J.J., A knowledge-based approach in designing combinatorial or medicinal chemistry libraries for drug discovery. 1. A qualitative

and quantitative characterization of known drug databases, *Journal of Combinatorial Chemistry*, **1(1)**, 55–68 **(1999)**

11. Herrick J.B., Peculiar elongated and sickle-shaped red blood corpuscles in a case of severe anemia, *The Journal of American Medical Association*, **312(10)**, 1063 **(2014)**

12. Ikuta T., Thatte H.S., Tang J.X., Mukerji I., Knee K., Bridges K.R., Wang S., Montero-Huerta P., Joshi R.M. and Head C.A., Nitric oxide reduces sickle hemoglobin polymerization: potential role of nitric oxide-induced charge alteration in depolymerisation, *Archives of Biochemistry and Biophysics*, **510(1)**, 53–61 **(2011)**

13. Ingram V.M., Gene mutations in human haemoglobin: the chemical difference between normal and sickle cell haemoglobin, *Nature*, **180(4581)**, 326–328 **(1957)**

14. Kato G.J., Piel F.B., Reid C.D., Gaston M.H., Ohene-Frempong K., Krishnamurti L., Smith W.R., Panepinto J.A., Weatherall D.J., Costa F.F. and Vichinsky E.P., Sickle cell disease, *Nature Reviews, Disease Primers*, **4**, 18010 **(2018)**

15. Kumari R. and Kumar R., Open Source Drug Discovery Consortium, & Lynn, A., g_mmpbsa--a GROMACS tool for high-throughput MM-PBSA calculations, *Journal of Chemical Information and Modeling*, **54(7)**, 1951–1962 **(2014)**

16. Lipinski C.A., Lombardo F., Dominy B.W. and Feeney P.J., Experimental and computational approaches to estimate solubility and permeability in drug discovery and development settings, *Advanced Drug Delivery Reviews*, **46(1-3)**, 3–26 **(2001)**

17. Mehanna A.S., Sickle cell anemia and antisickling agents then and now, *Current Medicinal Chemistry*, **8(2)**, 79–88 **(2001)**

18. Metcalf B. et al, Discovery of GBT440, an Orally Bioavailable R-State Stabilizer of Sickle Cell Hemoglobin, *ACS Medicinal Chemistry Letters*, **8(3)**, 321–326 **(2017)**

19. Miller B.R., McGee T.D. Jr., Swails J.M., Homeyer N., Gohlke H. and Roitberg A.E., MMPBSA.py: An Efficient Program for End-State Free Energy Calculations, *Journal of Chemical Theory and Computation*, **8(9)**, 3314–3321 **(2012)**

20. Morris G.M. and Lim-Wilby M., Molecular docking, Methods in Molecular Biology, Clifton N.J., **443**, 365–382 **(2008)**

21. Mpiana P.T., Tshibangu D.S., Shetonde O.M. and Ngbolua K.N., *In vitro* antidrepanocytaryactvity (anti-sickle cell anemia) of some congolese plants, *Phytomedicine: International Journal of Phytotherapy and Phytopharmacology*, **14(2-3)**, 192–195 **(2007)**

22. Muegge I., Heald S. L. and Brittelli D., Simple selection criteria for drug-like chemical matter, *Journal of Medicinal Chemistry*, **44(12)**, 1841–1846 **(2001)**

23. Oksenberg D., Dufu K., Patel M.P., Chuang C., Li Z., Xu Q., Silva-Garcia A., Zhou C., Hutchaleelaha A., Patskovska L., Patskovsky Y., Almo S.C., Sinha U., Metcalf B.W. and Archer D.R., GBT440 increases haemoglobin oxygen affinity, reduces sickling and prolongs RBC half-life in a murine model of sickle cell disease, *British Journal of Haematology*, **175(1)**, 141–153 **(2016)**

24. Oniyangi O. and Cohall D.H., Phytomedicines (medicines derived from plants) for sickle cell disease, *The Cochrane Database of Systematic Reviews*, **9(9)**, CD004448 **(2020)**

25. Pauling L. and Itano H.A., Sickle cell anemia a molecular disease, *Science* (New York, N.Y.), **110(2865)**, 543–548 **(1949)**

26. Piel F.B., Hay S.I., Gupta S., Weatherall D.J. and Williams T.N., Global burden of sickle cell anaemia in children under five, 2010-2050: modelling based on demographics, excess mortality and interventions, *PLoS Medicine*, **10(7)**, e1001484 **(2013)**

27. Piel F.B., Patil A.P., Howes R.E., Nyangiri O.A., Gething P.W., Dewi M., Temperley W.H., Williams T.N., Weatherall D.J. and Hay S.I., Global epidemiology of sickle haemoglobin in neonates: a contemporary geostatistical model-based map and population estimates, *Lancet* (London, England), **381(9861)**, 142–151 **(2013)**

28. Serjeant G.R., Sickle-cell disease, *Lancet* (London, England), **350(9079)**, 725–730 **(1997)**

29. Steinberg M.H., Hydroxyurea treatment for sickle cell disease, *The Scientific World Journal*, **2**, 1706–1728 **(2002)**

30. Trott O. and Olson A.J., AutoDockVina: improving the speed and accuracy of docking with a new scoring function, efficient optimization and multithreading, *Journal of Computational Chemistry*, **31(2)**, 455–461 **(2010)**

31. Van Der Spoel D., Lindahl E., Hess B., Groenhof G., Mark A.E. and Berendsen H.J., GROMACS: fast, flexible and free, *Journal of Computational Chemistry*, **26(16)**, 1701–1718 **(2005)**

32. Veber D.F., Johnson S.R., Cheng H.Y., Smith B.R., Ward K.W. and Kopple K.D., Molecular properties that influence the oral bioavailability of drug candidates, *Journal of Medicinal Chemistry*, **45(12)**, 2615–2623 **(2002)**

33. Yawn B.P., Buchanan G.R., Afenyi-Annan A.N., Ballas S.K., Hassell K.L., James A.H., Jordan L., Lanzkron S.M., Lottenberg R., Savage W.J., Tanabe P.J., Ware R.E., Murad M.H., Goldsmith J.C., Ortiz E., Fulwood R., Horton A. and John-Sowah J., Management of sickle cell disease: summary of the 2014 evidence-based report by expert panel members, *The Journal of American Medical Association*, **312(10)**, 1033–1048 **(2014)**.

(Received 08th October 2024, accepted 07th December 2024)